Computational Toxicology 32 (2024) 100334

Contents lists available at ScienceDirect

Computational Toxicology

journal homepage: www.sciencedirect.com/journal/computational-toxicology

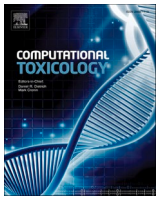

Full Length Article

Species specific kinetics of imidacloprid and carbendazim in mouse and rat and consequences for biomonitoring

Bohan Hu *, Ivonne M.C.M. Rietjens, Bert Spenkelink, Nico W. van den Brink

Division of Toxicology, Wageningen University and Research, Stippenneg 4, 6708WE, Wageningen, the Netherlands

ARTICLE INFO

Keywords:
Physiology based kinetic model
Species differences
Mouse
Imidacloprid
Carbendazim
Biomonitoring

ABSTRACT

This study aimed to develop physiologically based kinetic (PBK) models to predict the blood concentrations of imidacloprid and carbendazim and their primary metabolites 5-hydroxy-imidacloprid and 2-aminobenzimidazole after single or repeated oral exposure in mouse (*Mus musculus*), and compare this to corresponding kinetic data in rat (*Rattus norvegicus*). PBK model constants for conversion of imidacloprid and carbendazim and formation and clearance of their selected primary metabolites were quantified by *in vitro* mouse liver microsomal and S9 incubations. The performance of the newly developed PBK models was evaluated, based on a comparison to available literature data, showing that the models performed well. Predictions made were also compared to results from PBK model simulations for rats reported previously to obtain insight in species dependent differences in kinetics of these pesticides. The results thus obtained revealed substantial species differences in kinetics for these two pesticides between mouse and rat, especially for imidacloprid and to a lesser extent for carbendazim. Repeated dose PBK model simulations revealed that the models can facilitate estimation of external exposure levels under wildlife conditions based on internal blood concentrations of the parent compound. The rate of conversion and liver volume fraction were shown to influence the accuracy of these predictions with lower values providing less variable outcomes. It is concluded that PBK modeling provides a new approach methodology of use for wildlife biomonitoring studies and that results of the present study facilitate benchmarking of the species and compounds for which kinetics enable this with sufficient accuracy.

1. Introduction

Globally around two million tons of active pesticide ingredients are applied annually to prevent damages to crops, a number projected to increase to 3.5 million tons by the end of the 2020 s to meet the food demands of a growing world population [1]. While pesticides play an essential role in preventing weed overgrowth, fungal infestations, and insect and rodent plagues, they can also cause unwanted side effects in non-target species in the environment or in humans who may be exposed via food, ambient pesticide residues, or occupationally. Potential adverse outcomes can result in acute effects or delayed chronic effects, including compromised reproductive, immune, or nervous system functioning [2]. For imidacloprid, for instance, daily exposure at dose levels above 5 mg/kg BW/day for mouse could lead to immunosuppressive effects [3]. Another study [4] indicates that repeated daily dose levels over 15 mg/kg BW/day of imidacloprid could lead to hepatotoxicity and nephrotoxicity in mice. Studies have shown that long-term exposure to carbendazim can lead to adverse effects, including body weight loss and endocrine disruption [5,6]. Of all pesticides, insecticides and fungicides are most widely used in agriculture worldwide, followed by herbicides and rodenticides [7].

To ensure safe use levels of agrochemicals, regulatory agencies require a risk assessment, including hazard assessment and exposure quantification in the environment and for humans [8]. However, increasingly ethical, economic, and scientific arguments against using animal tests are raised in society and among scientists [9,10]. Since 2014, animal testing for scientific purposes has been strictly regulated within the EU, under EU directive 2010/63/EU [11]. The directive provides the legal framework for the '3R' principle, introduced first by Russel and Burch (1959), which aims for Replacement of animal testing with non-animal methods, Reduction of the number of test animals to obtain valid results, and Refinement of practices to minimize the suffering of animals [12].

Considerable progress has been made towards the incorporation of alternative testing strategies in hazard assessment by using *in vitro* assays with cells or lower organisms (e.g., invertebrate testing or the

* Corresponding author.
E-mail address: bohan.hu@wur.nl (B. Hu).

https://doi.org/10.1016/j.comtox.2024.100334
Received 15 July 2024; Received in revised form 11 October 2024; Accepted 13 October 2024
Available online 18 October 2024

zebrafish embryo test) in order to better understand the mode of action of a chemical or to derive *in vitro* concentration–response curves that can be translated to *in vivo* dose response curves using physiologically based kinetic (PBK) modeling facilitated reverse dosimetry [13,14]. While PBK models have received increasing attention to facilitate the 3Rs in hazard characterization [15], their primary application in exposure assessment has mainly focused on route-to-route extrapolation in humans, for example, between oral and inhaled doses [16,17], reverse dosimetry from biomarkers to oral doses [18–22], or the interspecies extrapolation from dose levels in experimental animals to human equivalent dose levels [23–25]. In line with these applications, there may be potential to incorporate PBK modeling into the biomonitoring of pesticide exposures in wildlife as well. Currently, environmental exposure assessment in wildlife species is often more challenging than for humans due to the complexity of environmental exposure routes, the unknown time between exposure and analysis and a multitude of receptor species, while typically still requiring invasive tissue samples [26]. PBK modeling-based extrapolation from data on non-lethal samples, like blood internal concentrations, to external oral doses may facilitate wildlife exposure modeling.

However, it is a known fact that different species can have variations in their physiology and metabolism, which can result in differences in the way they process and eliminate chemicals from their bodies. This can make it challenging to apply general PBK models to predict the toxicokinetic of chemicals across different species. To address this issue, it is important to assess species-specific kinetic constants, to define species-specific PBK models. By incorporating species-specific data into the models, researchers can account for the unique characteristics and traits of each species and obtain more reliable predictions of the relationship between external dose levels and internal exposures (and vice versa) for specific species. Overall, understanding the differences between species and how these differences impact the kinetics of chemicals is essential for developing effective PBK models that can be applied across various species. Therefore, this study sets out to develop mouse specific PBK models for the neonicotinoid pesticide imidacloprid and the fungicide carbendazim and to compare the predictions made to those obtained by earlier developed PBK models for rats [27], using similar approaches. These PBK models previously developed for the rat (*Rattus norvegicus*) were verified based on a comparison of the predictions made to available literature data [27]. In the current study, PBK models are developed for the same compounds for the mouse (*Mus musculus*), another rodent receptor species, allowing interspecies comparison. The results of this comparison will help identify the need for species-specific PBK models. Overall, the study seeks to contribute to developing more effective PBK models and a better understanding of how these can be applied across a range of species and reduce the need for invasive animal testing in wildlife biomonitoring.

2. Material and methods

2.1. Chemicals

Imidacloprid (CAS-No.1338261–41-3, purity 99.8 %), 5-hydroxy-imidacloprid (CAS-No.380912–09-4, purity 99.8 %), carbendazim powder of analytical standard (purity 98 %, CAS 10605–21-7) and 2-aminobenzimidazole (Pestanal® analytical standard, CAS 934–32-7) were purchased from Sigma-Aldrich (Schnelldorf, Germany) and dimethyl sulfoxide (DMSO) from Merck (Darmstadt, Germany). Uridine 5′-diphosphate-α-D-glucuronic acid (UDPGA), was obtained from Sigma-Aldrich. NADPH (β-nicotinamide adenine dinucleotide phosphate, reduced form, tetrasodium salt) (– min 95 %, CAS-No.2646–71-1), was purchased from Biosynth Carbosynth Group (Compton, United Kingdom). Pooled male mouse liver microsomes (CD-4) and pooled male mouse liver S9 were purchased from Croning (Glendale US).

2.2. PBK model development

PBK models can be utilized to forecast the time dependent changes in the concentration of a substance in the bloodstream or target organs at a specific dosage and vice versa. For small mammals, the oral exposure pathway is typically the most prevalent for pesticides. Constructing a PBK model involves several key steps: (1) Developing a conceptual PBK model framework that incorporates all necessary absorption, distribution, metabolism (Fig. 1), and excretion (ADME) processes and related compartments; (2) acquiring data on the physiology of the targeted species, in this study the mouse, and on the physicochemical attributes of the focal chemicals (imidacloprid and carbendazim); (3) quantifying the various ADME parameters that influence the internal kinetics, including uptake through the gastrointestinal system, distribution to the various target organs, metabolism in different organs (often primarily the liver), and processes of elimination. In formulating the PBK model, each organ of interest is treated as a distinct segment for which the kinetic processes are described by its own differential equation. The transport of chemicals throughout the organism occurs through the bloodstream, also characterized by a unique differential equation. Once the model is defined this is followed by (4) evaluation of its performance by comparison to available *in vivo* data and a sensitivity analysis. Once evaluated and shown adequate (5) the model can be used to make predictions.

The conceptual framework of the PBK models for mouse, specifically for imidacloprid and carbendazim, is depicted in Fig. 2. These models include distinct tissues such as the liver (principal site for metabolism), kidneys, small and large intestines, adipose tissue, and arterial and venous bloodstreams. The remaining internal organs are grouped together as a rapidly-perfused tissue compartment, while other body parts like the skin, muscles, and bones are aggregated into a slowly-

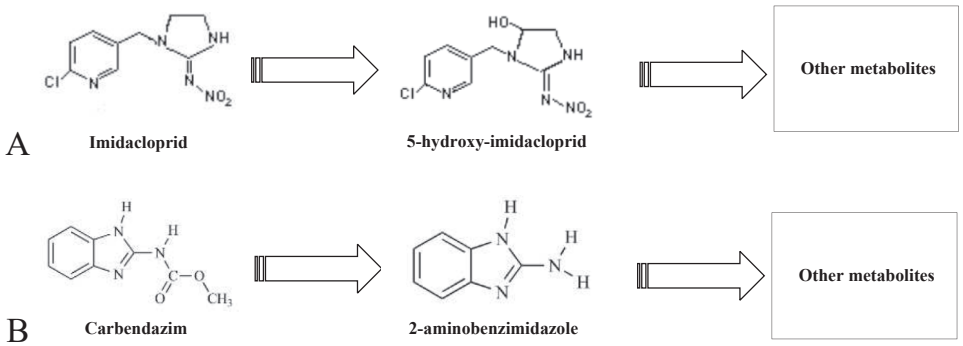

Fig. 1. Selected metabolic pathway of imidacloprid and carbendazim in mouse based on the pathways described in rat [41,47]. After oral uptake, imidacloprid is mono-hydroxylated to 5-hydroxy-imidacloprid, and then 5-hydroxy-imidacloprid is further converted into other metabolites (pathway A), and carbendazim is metabolized to 2-aminobenzimidazole, which is then further converted into other metabolites (pathway B).

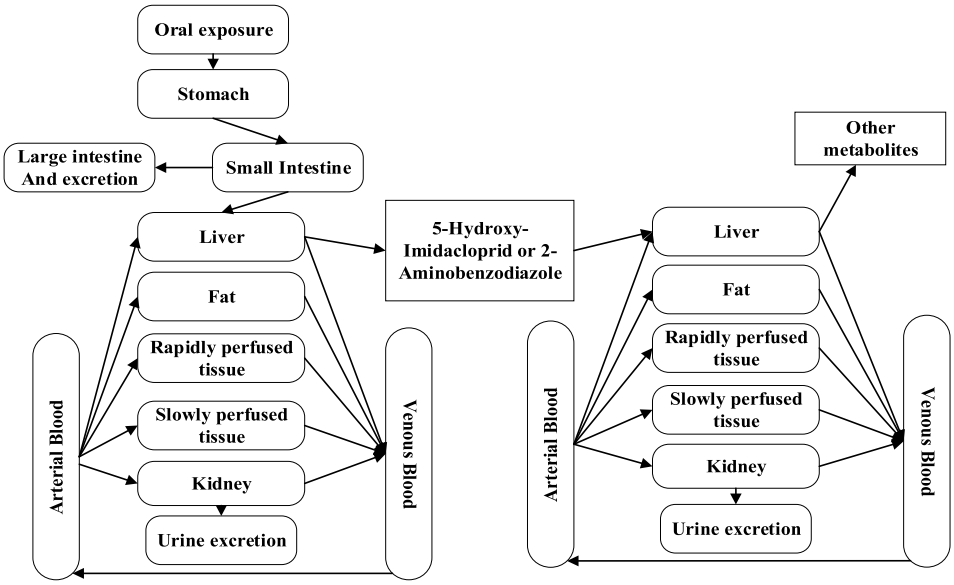

Fig. 2. Schematic presentation of the mouse carbendazim and imidacloprid model with a sub model for their primary metabolites 5-hydroxy-imidacloprid and 2-aminobenzoiazole.

perfused tissue segment. Additionally, to facilitate the measurement of blood concentrations of the key metabolites over time, the PBK models incorporate a sub model for these primary metabolites that encompasses only the internal organs, excluding the intestines (as illustrated in Fig. 2). Key physiological constants in the model, such as the rate of blood flow and the weight ratio of organ compartments, were derived from existing literature [28,29]. Cardiac output (QC) was calculated from the empirical algorithm by Arms & Travis (1988) as QC = 16.5* BW 0.74, and blood flow rates to organs were determined from the percentages of cardiac output given by Brown et al. [29]. Notably, these blood flow rates only represent resting animals while postural change, movement, or feeding may significantly increase the blood flow to skeletal muscle or the GI tract [29]. For simplicity, such changes in blood flow distribution are not accounted for in the current model. Moreover, cardiac output and organ volumes were only determined for male animals as there were insufficient data to account for intersex differences typically existing in mammalian species [29].

After being ingested orally, the substance first passes through the stomach and then into the small intestine. The transfer of imidacloprid and carbendazim from the stomach to the small intestine was described as a first-order process. In the small intestine, the uptake of imidacloprid and carbendazim is characterized using first-order kinetics. The non-absorbed part of the compounds was modelled to be transported into the large intestine and excreted. All absorbed imidacloprid and carbendazim were assumed to be transferred directly to the liver compartment via the portal vein. Tissue and plasma partition coefficients were estimated based on the method of [28], (see Appendix 3). The rate constant for intestinal absorption was derived from the Papp (apparent permeability constant) values which were previously determined in *in vitro* transport experiments with Caco-2 cells and amounted for imidacloprid and carbendazim to $3.98*10^{-5}$ cm/s (standard deviation: $5.50*10^{-6}$, n = 9 wells) and $7.76*10^{-5}$ cm/s (standard deviation: $3.09*10^{-6}$, n = 9 wells), respectively [27].

The elimination of imidacloprid and carbendazim in the model is achieved through liver metabolism, involving phase I mediated transformation as measured in liver microsomal tests, detailed subsequently, and via renal clearance through glomerular filtration. The choice of phase I metabolites for the PBK sub-model, specifically 5-hydroxy-imidacloprid and 2-aminobenzamidazole, was informed by prior *in vivo* rat studies [30,31], which identified these as significant primary metabolites, and also by their prevalence in the mouse liver microsomal incubations of the present study (see Results section for details). Considering the incomplete understanding of the metabolic routes for 5-hydroxy-imidacloprid and 2-aminobenzamidazole, their further metabolism in the model was simulated using depletion kinetic constants derived from liver S9 incubations. These incubations included NADPH and UDPGA as co-factors to facilitate both continued phase I and phase II primary metabolic processes.

The kinetic constants for depletion of the parent compound and the formation and depletion of the selected major metabolites 5-hydroxy-imidacloprid and 2-aminobenzimidazole were quantified based on *in vitro* incubation methods. All kinetic rate constants expressed in nmol/min/mg protein, were scaled to the liver compartment based on known hepatic microsomal or S9 protein concentrations (Table 1), respectively [32–36]. The liver weight was scaled based on liver to body weight ratios [29].

Since the distribution of imidacloprid and carbendazim among mouse tissues has not been previously studied experimentally, QSAR-derived values were used to predict the *in vivo* distribution of imidacloprid and carbendazim within the body [28]. Algorithms providing species-specific parameters were considered because they have been used previously in mouse PBK models [37]. Imidacloprid and carbendazim partition coefficients were calculated according to the approach described by DeJongh et al. [28] using mouse data whenever possible, and, where not applicable, rat data were used instead. An overview of the QSARs, including central equations and input parameters, can be found in Appendix 3, or in the cited publications. In case the QSARs did not provide algorithms for all required tissues, missing partition coefficients were assumed to be similar to those of available tissues (e.g. liver and richly-perfused tissue).

The model's code is detailed in the supplementary materials in Appendix 1 and 2. Berkley Madonna was used for data processing and model code running (Berkeley Madonna v.9.2.2 (Macey and Oster, UC Berkeley, CA). The efficacy of the model was ascertained by aligning the PBK model's output with existing *in vivo* empirical data from prior studies using the same BW and dose levels for the predictions as used in the *in vivo* studies.

2.3. *In vitro mouse liver microsomal and S9 incubations*

The rates of hepatic metabolism of the parent compounds and the formation of their primary phase I metabolites were assessed by *in vitro*

assays, using incubations with mouse liver microsomes. Mouse liver microsomes were incubated with imidacloprid or carbendazim, resulting in depletion of the parent compounds and the formation of phase I metabolites. The experimental protocol was optimized to ensure that all experiments were conducted at protein concentrations and incubation times showing linear responses in metabolic rates. Metabolites were identified and quantified by comparing occurring peaks and peak areas in the UPLC patterns of the *in vitro* incubations with those of commercially available standards. The optimized incubation mixture consisted of (final concentrations) 2 mg/mL male CD-1 mouse liver microsomal protein plus 5 μM NADPH as cofactor in 10 mM potassium phosphate (pH 7.4) in a total volume of 200 μL. After a short pre-incubation in a shaking water bath at 37 ℃, the metabolic reaction was initiated by addition of the parent compounds at final concentrations of 0, 50, 100, 200, 300, and 400 μM (added from 100 times concentrated stock solutions in DMSO, keeping the final DMSO concentration in the incubations at 1 %). Control samples consisted of incubations without co-factor addition. The samples were incubated for 60 min for both compounds in a shaking water bath at 37℃, after which the metabolic reactions were terminated by adding 200 μL ice-cooled acetonitrile (1:1 v/v). Samples were vortexed and centrifuged for 5 min at 14,000 g and 4℃, and aliquots of 50 μL were taken for UPLC analysis.

The kinetic rate constants for the degradation of the primary metabolites, 5-hydroxy-imidacloprid and 2-aminobenzimidazole, were determined in experiments using incubations with mouse liver S9 fractions, supplemented with NADPH and UDPGA. This setup was designed to encompass both phase I and phase II metabolic reactions. The experimental conditions were fine-tuned to ensure a linear relationship between substrate depletion and incubation duration and S9 protein concentration. The final incubation mixtures consisted of 20 mg/ml S9 protein, 2 mM UDPGA, and 7.5 mM NADPH in 0.1 M potassium phosphate (pH 7.4), making up a total volume of 200 μL. The reactions were initiated by adding the substrate after a 1-minute preincubation at 37 °C, and the samples were then incubated for 120 min. To terminate the reaction, 200 μL ice-cold acetonitrile was added, samples were vortexed and centrifuged for 5 min at 14,000 g and 4℃, and aliquots of 50 μL were taken for UPLC analysis [38].

The standard Michaels-Menten regression model was applied to assess metabolic rates and quantify the kinetic constants (equation 1)

$$v = (Vmax^{*}S)/(Km + S)$$

where v (nmol/min/mg protein) represents the rate of substrate depletion or product formation, V_{max} (nmol/min/mg protein) denotes the maximum rate of substrate depletion or product formation, S (μM) signifies the substrate concentration, and Km (μM) stands for the apparent Michaelis Menten constant, the substrate concentration where v equals 0.5Vmax.

2.4. Chemical analysis

Carbendazim and imidacloprid incubation samples were analyzed with an Ultra Performance Liquid Chromatography (UPLC) system (Waters Acquity, H class, Breda, Netherlands) and a UV-DAD (ultraviolet-diode array detector) (Waters, Milford, MA, USA), equipped with an analytical BEH type C-18 column of dimensions 2.1 x 50 mm (Waters Acquity). The mobile phase consisted of a gradient made with nanopure water with 0.1 % trifluoroacetic acid (A) and 10 % acetonitrile in nanopure water (B). The elution was gradually increased in five steps of each 2 min from 0 % to 100 % A, at a flow rate of 0.6 mL/ min (3480 Pa, 40 °C). Chromatograms were obtained from Empower chromatographic software (version 3). Imidacloprid and carbendazim and their metabolites in the samples were identified by comparison of the peak retention time and UV/Vis spectra with the peak retention time and UV/Vis spectra of the external standards. Absorption was measured at 270 nm and 280 nm for imidacloprid and its metabolites, and carbendazim and its metabolites, respectively, and linear calibration curves were generated from the analytical standards for quantification based on peak areas.

2.5. Sensitivity analysis

A sensitivity analysis was performed to elucidate the sensitivity of the PBK model predictions to the various model parameters and quantify which parameters influence the model predictions most. The influence of an increase of 5 % of each parameter on the predicted maximum blood concentration (C_{max}) for imidacloprid or carbendazim was quantified in the sensitivity analysis. Sensitivity coefficients (SC) were assessed by using the following equation:

$$SC = (C' - C)/(P' - P)x(P/C)$$

where C is the initial value of the model output with an initial set of parameters (i.e., C_{max} in blood); C' is the modified model output resulting from a specific increase of the value of the parameter value of interest; P is the initial parameter value; P' is the modified parameter value (Evans and Andersen 2000). A 5 % increase in parameter values (P → P') was used to analyze the effect of a change in parameter values on the C_{max} of imidacloprid and carbendazim at a dose of 20 mg/kg BW and 1000 mg/kg BW, respectively, representing the dose levels used in the available *in vivo* studies used for model evaluation [30].

2.6. Comparisons between the two species (mouse and rat)

Finally, the kinetic constants and predicted time and dose dependent blood concentrations for mouse were compared with those obtained by previously reported PBK models for rat [27] to quantify and understand potential species dependent differences. To this end PBK model prediction for single as well as repeated oral dose regimens were compared.

3. Results and discussion

3.1. In vitro metabolic rates

A representative chromatogram of incubations of imidacloprid with mouse liver microsomes is shown in Appendix 3. Based on this, 5-hydroxy-imidacloprid was identified as the primary metabolite of imidacloprid. The main metabolite of carbendazim, detected in the supernatant of the *in vitro* incubation of carbendazim with mouse liver microsomes was 2-aminobenzimidazole (Appendix 3).

In this study, PBK models for imidacloprid and carbendazim were developed to simulate the time-resolved concentrations of these compounds in mouse blood following both single and repeated dose exposures, extending the analysis to include interspecies comparisons with rats, as detailed in prior research [27]. These models include kinetic parameters for the metabolism of carbendazim and imidacloprid, alongside their primary metabolites, identified through *in vitro* mouse hepatic microsomal and S9 incubations. Notably, these substances were rapidly metabolized in incubations with male mouse liver microsomes, yielding significant phase I metabolites such as 5-hydroxy-imidacloprid and 2-aminobenzimidazole, products of hydroxylation and hydrolytic cleavage, respectively [30,39]. Fig. 3 highlights the substrate concentration-dependent rates for the depletion of imidacloprid and carbendazim, and the formation of their major metabolites in incubations with mouse liver microsomes and S9 fractions. The detailed kinetic parameters derived from these data, including Km and Vmax values for depletion and formation, are presented in Table 2. This comprehensive approach not only advances our understanding of the metabolic processing of these compounds in mice but also facilitates a comparative analysis with rat data, thereby enhancing the model's applicability for interspecies extrapolation and the evaluation against *in vivo* data [30,31,40].

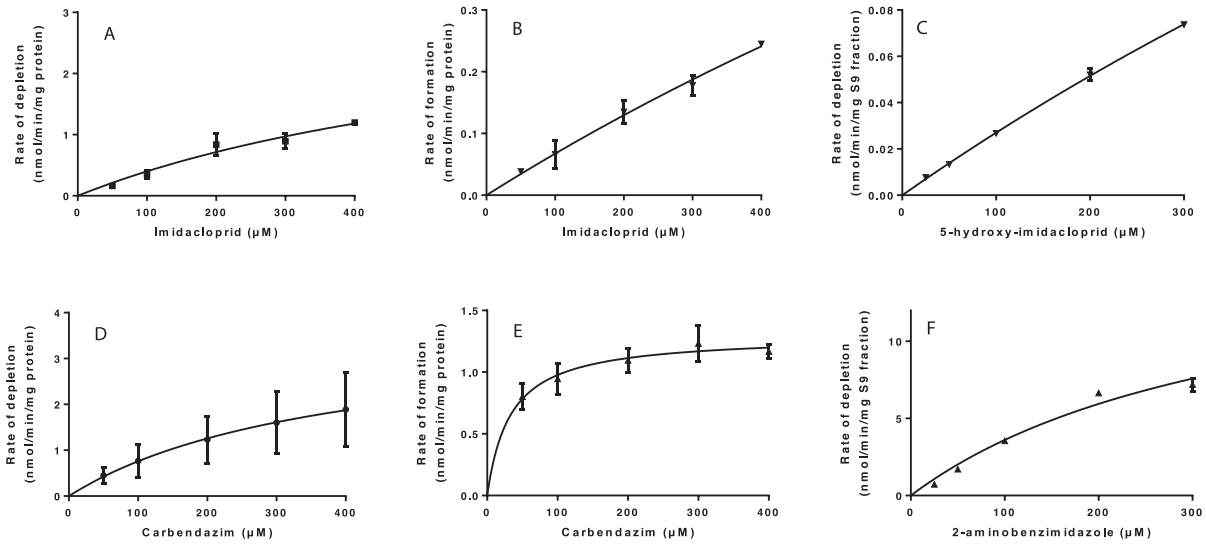

Fig. 3. Concentration-dependent rate of imidacloprid depletion (A) 5-hydroxy-imidacloprid formation (B) and depletion (C) in incubations with mouse liver microsomes (A,B) and S9 fractions (C) and concentration-dependent rate of carbendazim depletion (D) and 2-aminobenzimidazole formation (E) and depletion (F) in incubations with mouse liver microsomes (D,E) and S9 fractions (F).Each data point represents the average and standard deviation of n = 3 independent measurements.

Results of the present study reveal that the imidacloprid metabolism in incubations with mouse hepatic samples resulting in formation of 5-hydroxyimidacloprid as the major metabolite is qualitatively similar to what was previously reported for rats [27,41]. Previous studies on the biotransformation of carbendazim in rats have shown that rodents also share similar metabolic pathways for carbendazim, with 2-aminobenzimidazole as the main metabolite [30]. For carbendazim, additional peaks that may belong to hydroxylated products of carbendazim, a further breakdown product of 2-aminobenzimidazole [42] were detected (see Appendix 3). However, the identification and further characterization of these peaks was beyond the scope of this study.

The V_{max} values for the depletion of imidacloprid and carbendazim by mouse liver microsomes were relatively similar, at 3.41 ± 1.4 and 3.67 ± 2.1 nmol/min/mg microsomal protein, respectively (Table 2). The Km for the depletion of imidacloprid by mouse liver microsomes was twice the one for carbendazim, being 753 and 383 μM, respectively. Similarly, the maximum formation rates, V_{max}, for 5-hydroxy-imidacloprid and 2-aminobenzimidazole were comparable at 1.73 and 1.28 nmol/min/mg protein, respectively. However, the Km differed being 2466 and 33 μM for formation of 5-hydroxyimidacloprid and 2-aminobenzimidazole respectively. The V_{max} for depletion of 5-hydroxy-imidacloprid and 2-aminobenzimidazole were 2.6 and 16.9 nmol/min/mg S9 protein. The Km of the depletion rate of 5-hydroxy-imidacloprid is much smaller than that for 2-aminobenzimidazole by mouse liver S9 fraction, at 85 and 369 μM.

3.2. Model evaluation

For evaluation of the mouse PBK models, only a single study on carbendazim was available which provides time resolved amounts of the parent compound in blood of nude mouse (25 g body weight), after an oral dose of 500 mg/kg BW carbendazim and expressed as percentage of the oral dose [30]. Fig. 4 presents the comparison between these reported *in vivo* data and the mouse carbendazim PBK model simulation results for the amount of carbendazim in the blood compartment expressed as a percentage of the total dose after a single oral exposure of

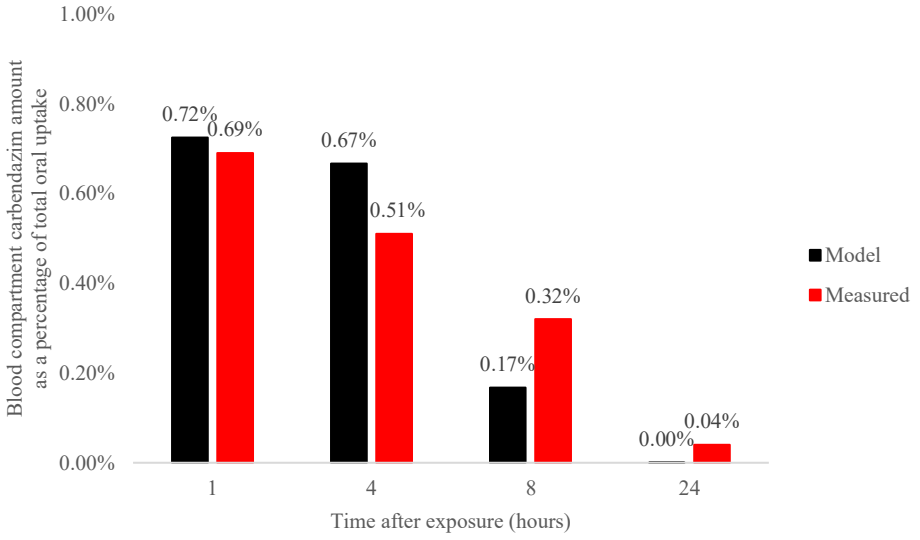

Fig. 4. Model calculated (black) and measured (red) carbendazim blood amount in mice as a percentage of total dose after a single oral dosing with 500 mg/kg BW [30]. (For interpretation of the references to colour in this figure legend, the reader is referred to the web version of this article.)

500 mg/kg BW.

Carbendazim blood levels following the oral dose were well predicted (Fig. 4). Due to the absence of relevant *in vivo* studies on imidacloprid in mice, the mouse imidacloprid PBK model could not be verified using mouse kinetic data. However, a similar rat PBK model previously showed adequate predictions for rat [27]. This implies that the confidence in the mouse model for imidacloprid is based on i) the fact that the model for rat and mice using species specific constants both predicted adequately for carbendazim, verifying the read-across from rat to mouse, and the fact that ii) the verified rat model for imidacloprid was converted into a mouse model in the same way for imidacloprid as shown valid for carbendazim.

Fig. 5 presents the mouse PBK model based predictions of imidacloprid, carbendazim, 5-hydroxy-imidacloprid and 2-aminobenzimidazole blood concentrations upon various single oral dose levels, over a 24 h period following dosing. The absorption of imidacloprid was rapid at all dose levels, with the maximum blood concentrations being reached within the first hour after dosing (Fig. 5A). With increasing dose levels, the Cmax of the parent compound increased linearly with the dose up to at least 125 mg/kg BW. The clearance from the blood showed a monophasic decline, with the concentration dropping to less than 10 % of the Cmax within the first 8 h following exposure. Carbendazim exhibited a similar rapid absorption, with peak blood concentrations occurring within 2 h post-dose across all dose levels (Fig. 5B). Also for carbendazim the Cmax of the parent compounds increased linearly with the dose up to at least 125 mg/kg BW. The elimination phase for carbendazim was also comparable to that for imidacloprid. For the metabolites 5-hydroxy-imidacloprid and 2-aminobenzimiazole, peak concentrations were observed within the first hours (Fig. 5C,D). The decline in the metabolite concentrations was rapid post-peak, due to efficient subsequent clearance of these primary metabolites by metabolism and excretion. With increasing dose levels, the Cmax of the metabolites did not increase linearly with the dose, suggesting a saturation of the metabolite formation process, which was particularly evident for the conversion of carbendazim to 2-aminobenzimidazole, likely due to the saturation of its formation (Fig. 3E). Figure E and F present the time dependent change in the ratio between the metabolite and parent compound concentration. These results reveal that for imidacloprid, at dose levels < 50 mg/kg BW thisratio increases rapidly in the first hours after which it reaches a constant value. It is also shown that this ratio is hardly influenced by the dose, while it starts to deviate somewhat more, taking more time to reach the constant value, when the dose increases further. Meanwhile for carbendazim, the effect of dose on this ratio is more pronounced at all dose levels. This result reveals that for

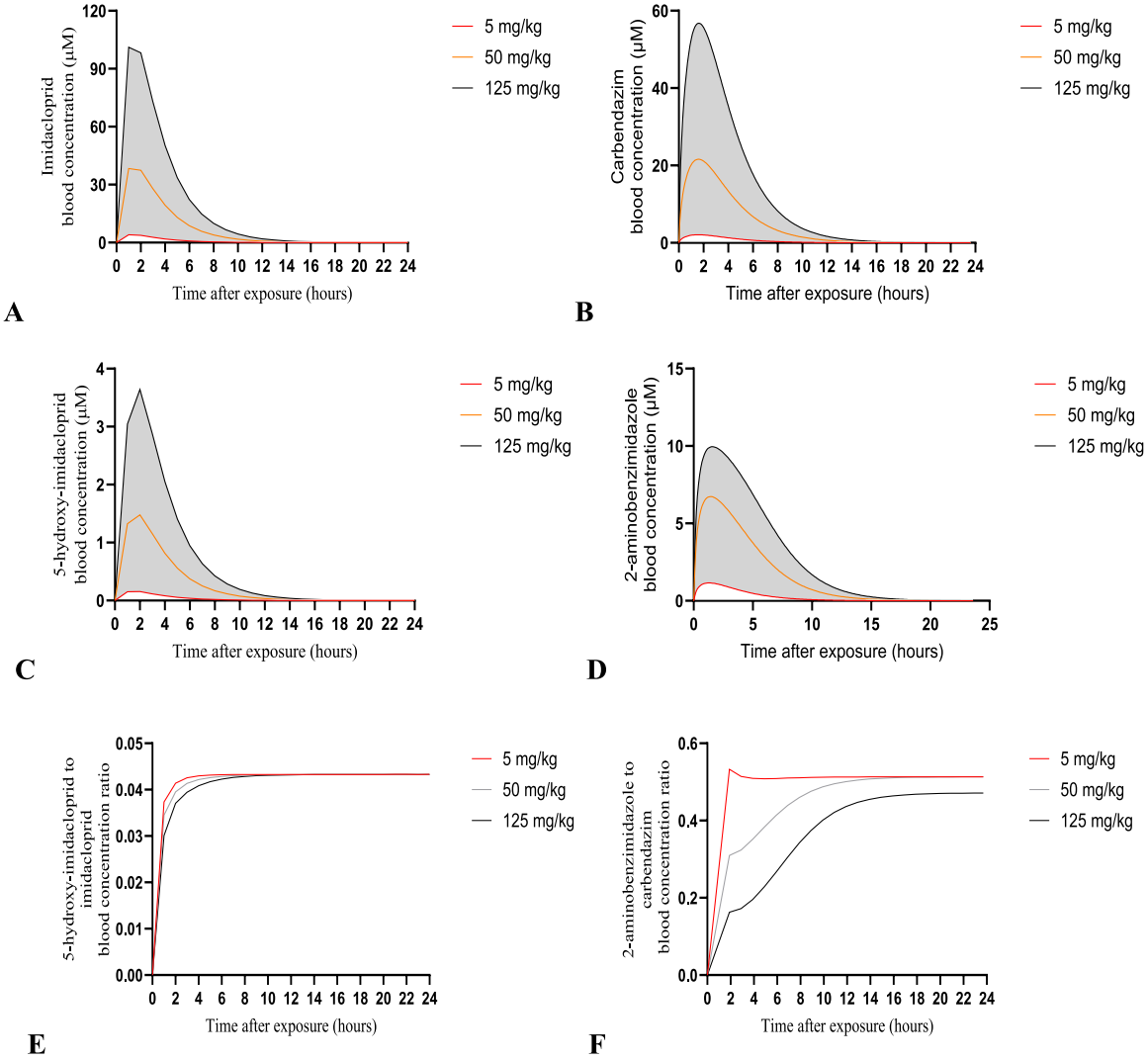

Fig. 5. Mouse PBK model based prediction of (A) imidacloprid and (C) 5-hydroxy-imidacloprid blood concentration vs exposure time upon exposure to imidacloprid, at an oral dose of 5, 50 and 125 mg/kg BW, and a fixed body weight of 25 g and (B) carbendazim and (D) 2-aminobenzimidazole blood concentration vs exposure time upon exposure to carbendazim, at an oral dose of 5, 50 and 125 mg/kg BW, and a fixed body weight of 25 g. (E) and (F) present the concentration ratio of metabolite to parent compound in blood after single exposure under different dose levels.

imidacloprid the ratio metabolite/parent compound is mainly influenced by the time since dosing and less by the dose level so that this ratio can be used to estimate the time following dosing, especially in the first hours following dosing. For carbendazim exposure in mouse the ratio appears to be influenced by both time after dosing and dose level so that it can not be used to estimate the time since dosing.

3.3. Sensitivity analysis

Fig. 6A and 6B present the results of a sensitivity analysis for the mouse PBK model predicted maximum blood concentration (C_{max}) for imidacloprid and carbendazim.

For imidacloprid, the analysis reveals that the maximum velocity for metabolism in the liver (Vmax0) had the highest positive normalized sensitivity coefficient, suggesting that the Cmax is most sensitive to changes in this parameter. The sensitivity of the model for changes in body weight (BW) and the Michaelis-Menten constant (Km) were less pronounced but positive, while the volume of the liver compartment (VLc) had a substantial negative effect. In the case of carbendazim, the sensitivity analysis showed the same parameters to be influential in the similar manner including VLc, Vmax0, and Km, while some additional parameters, including the volume of the slowly perfused tissue. (Vsc) and the flow constant from the systemic circulation to the liver (QLc) showed moderate positive sensitivity coefficients, indicating that increases in these parameters were associated with an decreased in Cmax.

3.4. Mouse model repeated exposures

Fig. 7 presents the blood concentration profiles for imidacloprid and carbendazim, along with their metabolites, upon repeated dose exposure at 5 mg/kg BW and 50 mg/kg BW, administered at 4-hour and 8-hour intervals for a 120 h period.

Both imidacloprid (Fig. 7A) and carbendazim (Fig. 7B) exhibited similar patterns in response to different dosing intervals. Administering a dose every 4 h resulted in higher steady state peak concentrations for both compounds compared to administering the same dose at 8-hour intervals. The shorter interval leads to less time for the compounds to be cleared from the body before a subsequent dosing, explaining the higher steady state level, while it also resulted in a less variable steady state concentration level. Meanwhile, the blood concentrations of 5-hydroxy-imidacloprid (Fig. 7C) and 2-aminobenzimidazole (Fig. 7D), were predicted to follow similar trends as those of their parent compounds. The shorter dosing interval of 4 h resulted in higher and less variable steady state concentrations of these metabolites. In contrast, the longer 8-hour interval allowed for more significant drops in concentrations between doses, due to more complete metabolism over the extended period. Notably, between both time intervals, the increase in the steady state levels of the parent compounds and their primary metabolites was linear with the dose, indicating that there was no saturation in the kinetics of the parent compounds, at these dose levels. This implies that these steady state concentrations can be used for reverse dosimetry to obtain estimates of the corresponding dose levels at an assumed dosing interval.

Fig. 7E and 7F, present the time dependent ratio of metabolite to parent compound derived from these concentration time profiles. Like the concentrations themselves also the ratios reach a steady state, with for both compounds, the 4-hour dosing interval resulting in less fluctuation in the metabolite-to-parent compound ratio, as indicated by the tighter oscillation of the lines. Conversely, the 8-hour interval displays more pronounced peaks and troughs, reflecting a wider time dependent variation in the blood concentrations due to the extended time between doses.

3.5. Interspecies comparison: Mouse model vs rat model

Fig. 8 presents the mouse and rat PBK model based predictions of the time dependent blood concentration of imidacloprid and carbendazim, and their metabolites, at 50 mg/kg BW a dose level where metabolism was shown not to be saturated and C_{max} and AUC increased linear with the dose. The Table in Appendix 3 presents a numerical overview of the C_{max}, T_{max}, and AUC values derived from these simulations for rat and mouse in the blood and liver compartment for imidacloprid, carbendazim, 5-hydroxy-imidacloprid and 2-aminobenzimidazole after single oral exposure to a dose of 50 mg/kg BW. From the comparison it follows that imidacloprid demonstrates a more pronounced interspecies difference between mouse and rats than carbendazim. Mouse reach peak blood concentration of imidacloprid quicker (lower T_{max}) (Fig. 3 and Appendix 3) and are predicted to display higher blood concentrations (C_{max}) of its metabolite 5-hydroxy-imidacloprid compared to rats. These interspecies differences can be ascribed to faster conversion of the parent compound to the primary metabolite in mouse. In contrast, the slower metabolism and uptake rate in rats result in a delayed C_{max} (higher T_{max}) for the parent compound and a lower C_{max} for the metabolite, resulting in prolonged exposure and slower clearance of imidacloprid in rats than mouse.

For carbendazim, the interspecies differences are less pronounced, and the concentration–time profiles of the parent compound in both species are relatively similar, with the variation being more pronounced in the metabolite profiles. The metabolite 2-aminobenzimidazole's blood concentration peaks somewhat sooner and reaches 2 fold higher levels in mouse (Fig. 9B and 9D). The AUC values for the parent compounds (see Appendix 3), which reflect overall exposure, are consistently higher in rats for both compounds, suggesting longer persistence due to somewhat slower clearance in this species.

Fig. 9 presents the species comparison of the blood concentration–time profiles for imidacloprid (Fig. 9A) and carbendazim (Fig. 9B) in rat and mouse models under repeated dosing of 50 mg/kg BW at 4-hour intervals over a 120-hour period. Both models predict that steady-state concentrations are reached within 24 h, with rats exhibiting higher steady state levels of imidacloprid than mouse, which can be

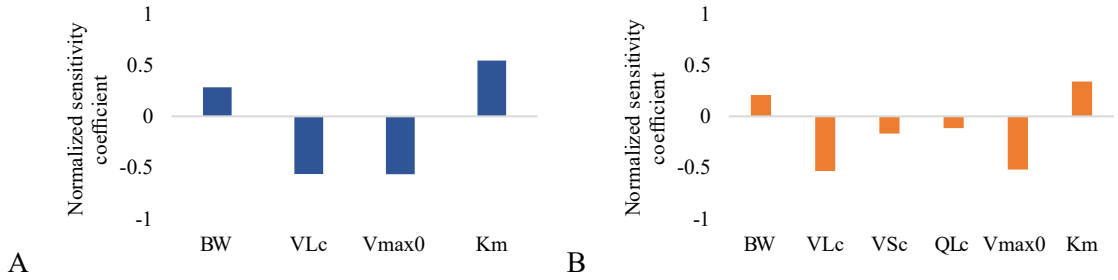

Fig. 6. Sensitivity analysis for the maximum blood concentration (Cmax) predicted by the mouse (A) imidacloprid of 20 mg/kg BW and (B) carbendazim of 1000 mg/kg BW, respectively. Sensitivity coefficients with a normalized value > 0.1 are presented. BW is body weight, Vlc is the volume of liver tissue, VSc is the volume of slowly perfused tissue, QLc is the liver blood flow, Vmax0 is the maximum depletion rate of imidacloprid/carbendazim in the liver compartment, Km is the Michaelis-Menten constant for the depletion of imidacloprid/carbendazim in the liver compartment.

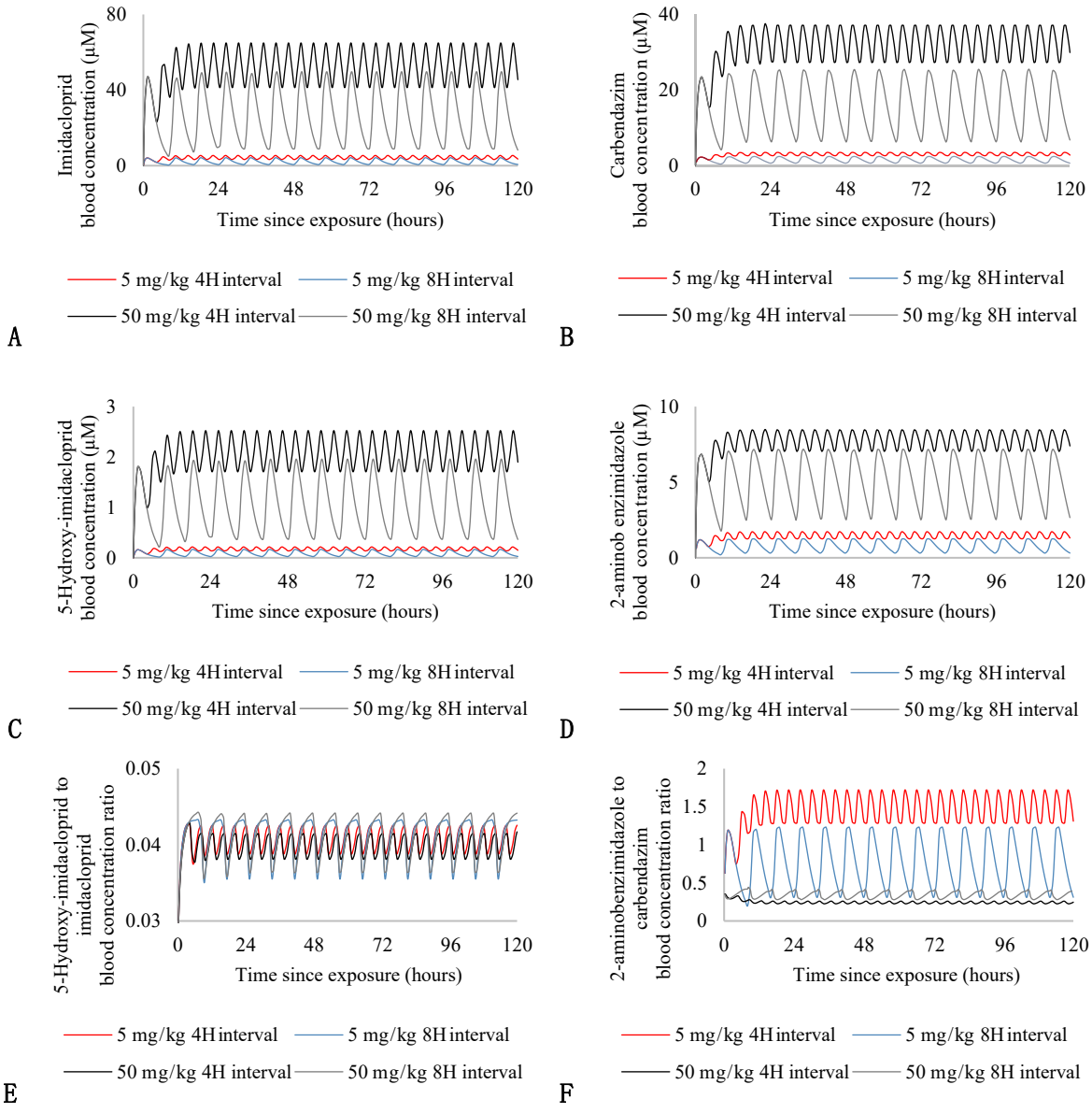

Fig. 7. Mouse PBK model calculated blood concentrations of (A&B) parent compounds and (C&D) primary metabolites, and (E&F) their ratio after repeated dose exposure at different dose levels and at dose intervals of 4 h (4H) and 8 h (8H), doses of 5 mg/kg BW and 50 mg/kg BW, and a fixed body weight 25 g.

ascribed to a more rapid metabolic clearance for imidacloprid in mouse than rat. For carbendazim the species difference in the blood concentration profile of the parent compound is limited. Also, for time dependent blood concentration profiles of the respective primary metabolites the species differences for carbendazim are less substantial than for imidacloprid. The faster metabolic clearance of imidacloprid in mouse results in higher steady-state levels for the resulting metabolite 2-hydroy-imidacloprid in mouse than rats.

In these scenarios involving repeated dosing, the interspecies comparisons also reveal that the variability in the steady-state blood concentration of imidacloprid is smaller for rats than mouse. This indicates that use of this steady-state level for reverse dosimetry in wildlife biomonitoring will result in more accurate results for rats than for mouse. For carbendazim the difference between the two species in variability in the blood concentrations is less than for imidacloprid.

3.6. Influence of PBK model parameters on accuracy of the wildlife biomonitoring

Given that the time dependent fluctuation in the steady state level will influence the accuracy of the wildlife biomonitoring it is of interest to characterize the effect of PBK model parameters on the variability in the steady state levels of the parent compounds. The sensitivity analysis already revealed the parameters for metabolism of the parent compounds VLc, Vmax0 and Km to be of influence on the predicted Cmax. Since catalytic clearance will increase with increasing Vmax and decrease with increasing Km, the best parameter to study this influence of catalytic clearance on variation in the predicted steady-state blood concentration levels is the catalytic efficiency kcat defined as the ratio Vmax0/Km. The VLc liver fraction represents the liver compartment where metabolism happens and was shown to be of influence with a negative sensitivity coefficient, indicating that an decreased in VLc will increase the blood concentration. Fig. 10 illustrates the fold differences between the maximum and minimum steady-state blood Cmax of imidacloprid and carbendazim predicted in rats and mouse under 4 h dose interval at variable kcat and liver volume fraction VLc. From these data it follows that the higher the catalytic efficiency the larger the fluctuation in the steady state level, and thus the less accurate the method for wildlife biomonitoring.

The results presented in Fig. 10A and 10B also reveal that another

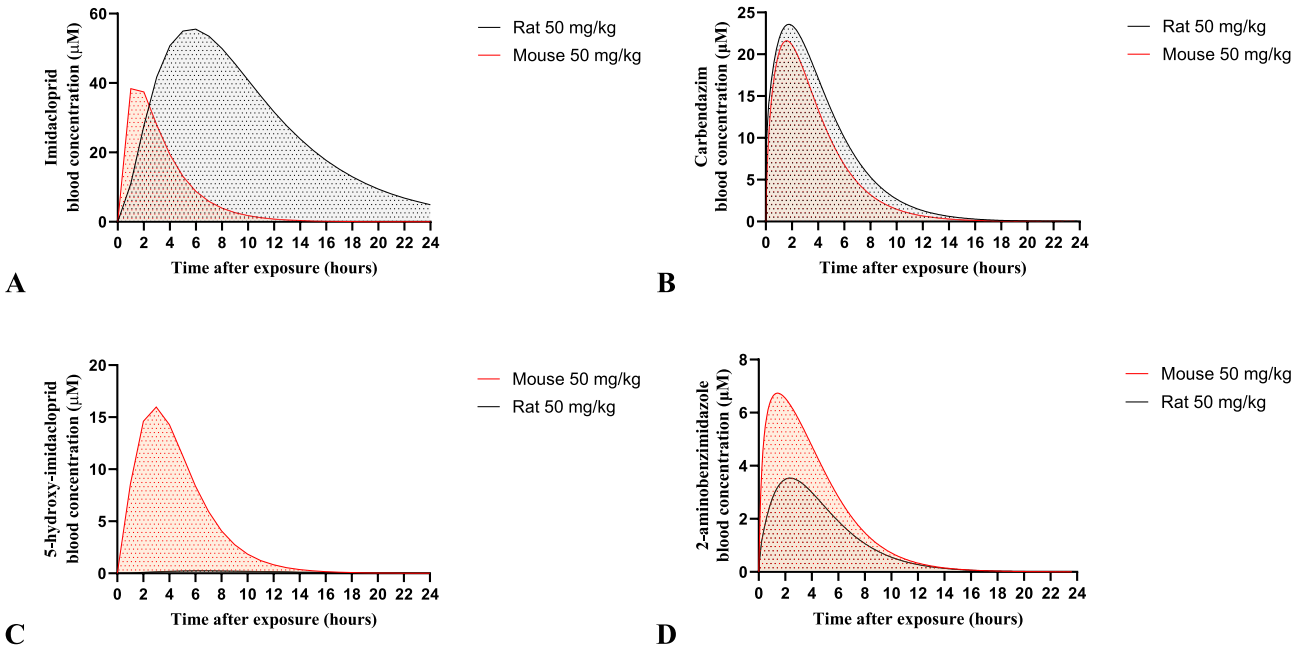

Fig. 8. Rat and mouse PBK model based predictions for the time dependent blood concentration of (A) imidacloprid, (B) carbendazim, (C) 5-hydroxy-imidacloprid, (D) 2-aminobenzimidazole, upon a single oral dose of 50 mg/kg BW.

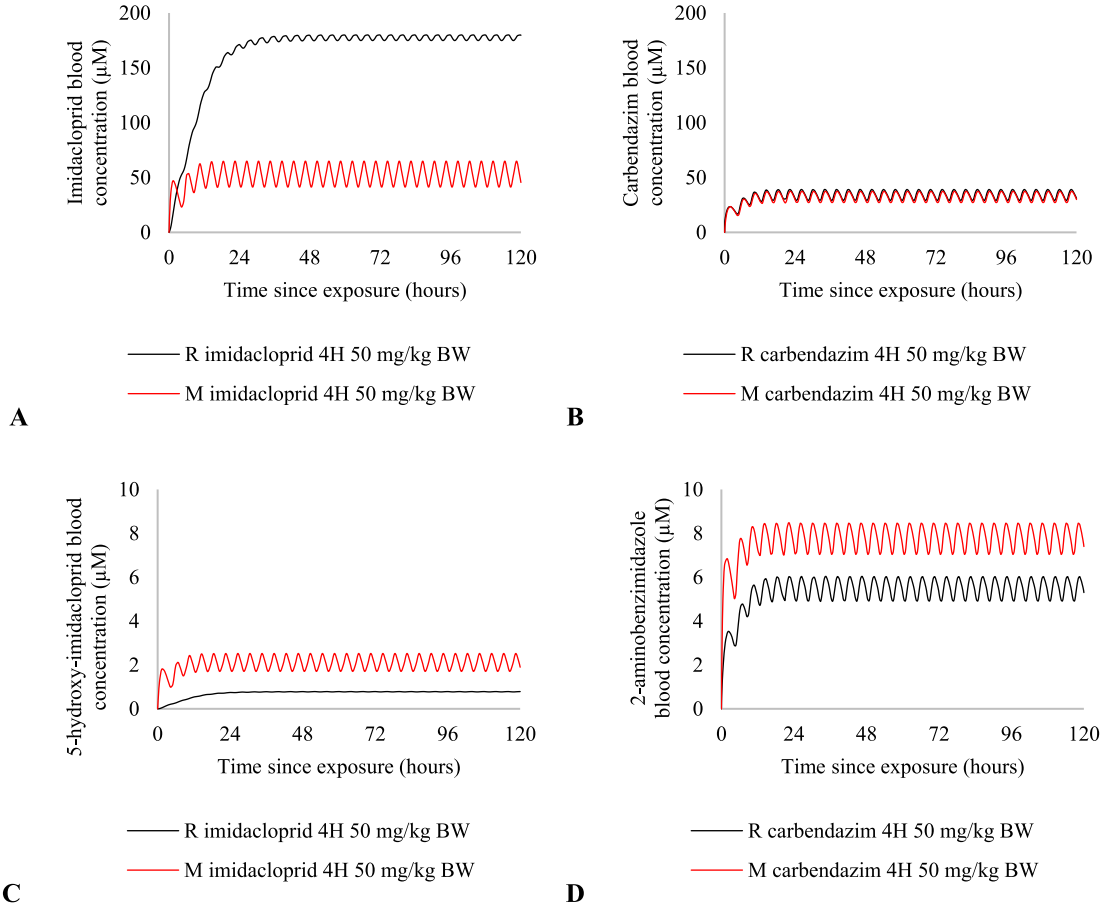

Fig. 9. Rat and mouse PBK model based predictions for time dependent blood concentrations of (A) imidacloprid, (B) carbendazim, (C) 5-hydroxy-imidacloprid and (D) 2-aminobendazimidazole, under a repeated dose level of 50 mg/kg BW, 4 h (4H) interval, fixed mouse body weight 25 g and rat body weight 165 g.

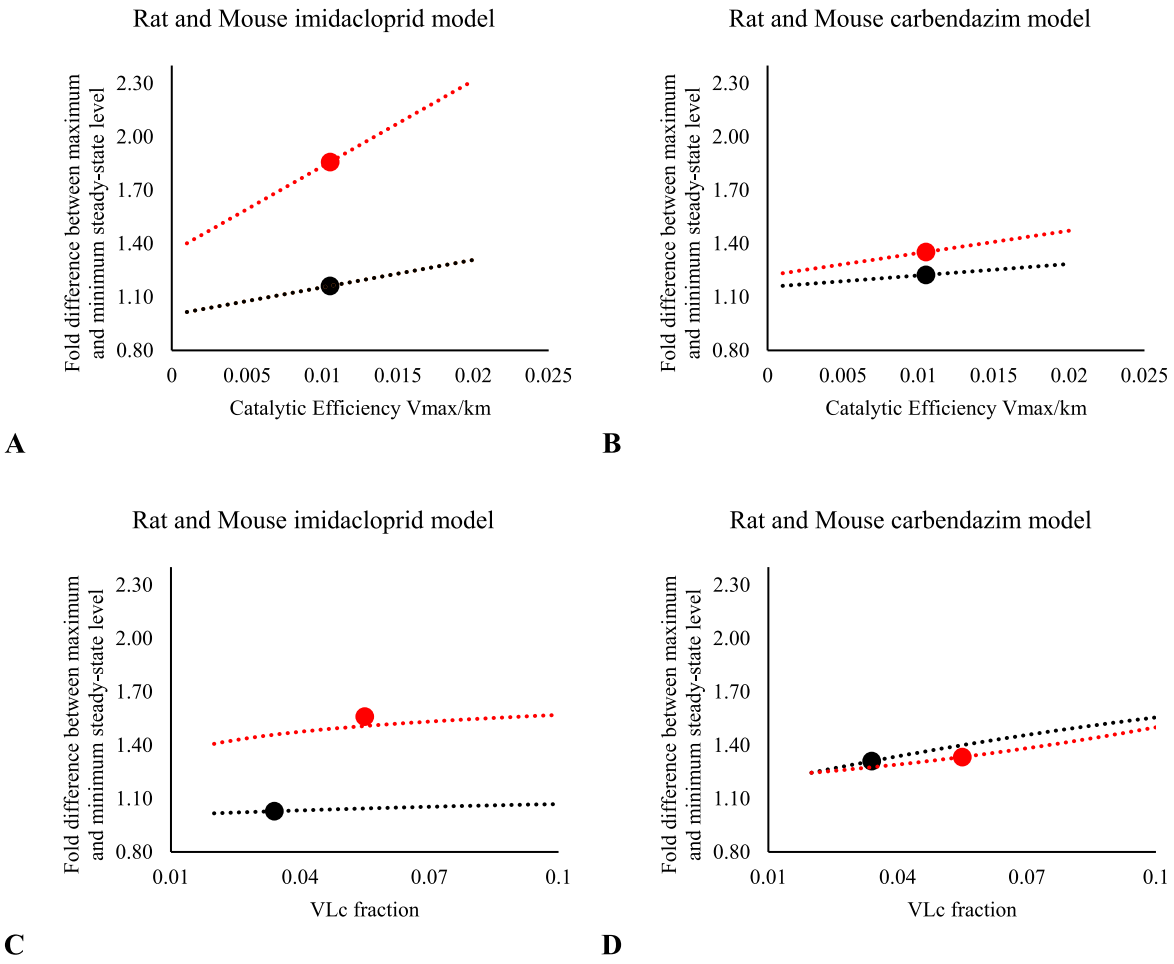

Fig. 10. The effect of (A,B) increasing kcat and (C,D) increasing VLc on the fold difference between predicted maximum and minimum steady-state blood concentrations of (A,C) imidacloprid and (B,D) carbendazim all at a dose of 50 mg/kg BW dose and 165 g (rat) / 25 g (mouse) body weight, and 4 h dose administration interval. Mouse model (red dots and lines) and rat model (black dots and lines). The dots present the values obtained using the actual parameters values for kcat and VLc as presented for the PBK models in Appendix 3, Table 1. (For interpretation of the references to colour in this figure legend, the reader is referred to the web version of this article.)

parameter is of influence given that for mouse at a given kcat the fold differences in the steady state levels are predicted to be for both compounds always higher than for rats. Based on the sensitivity analysis for the prediction of the blood Cmax of the parent compound (Fig. 6) this could be Vlc, which is 0.034 for rat and 0.055 for mouse (see Appendix 3, Table 1). Fig. 10C and 10D present the effect of a change in Vlc on the fold difference between the maximum and minimum predicted steady state levels of imidacloprid and carbendazim. This analysis corroborates that with increasing Vlc the fold difference also increases. Together these results indicate that, based on the VLc in the species of interest and the kinetics for metabolic clearance of a compound of interest one could upfront estimate whether PBK-model based reverse dosimetry would be an appropriate method for wildlife biomonitoring. A low VLc in combination with a low kcat together will result in slower clearance and thus more stable steady state levels for the blood concentration of the parent compound upon repeated dosing, because clearance in the time interval between dosing will be less efficient.

With respect to the quantitative formation of the primary phase I metabolites of imidacloprid and carbendazim, the kinetic rates within the experimental substrate range of 0 to 400 μM appeared to show species differences. The observed variations in the rates at which the parent substances are depleted and their primary metabolites are produced and eliminated could be due to the different enzymes that drive these metabolic reactions in the two species. Notably, mouse exhibit greater cytochrome P450 activity than rats [43], potentially resulting in more efficientmetabolism in mouse liver when this greater activity would relate to a P450 catalysing the respective conversion. The absorption and distribution of substances might also differ between the species due to varying physiological parameters, influencing the kinetics. For example, faster absorption will result in higher Cmax, and lower Tmax values, and a larger VLc will result in faster clearance and lower Cmax values when clearance is dominated by conversion in the liver [23,44].

PBK modelling can be considered a helpful tool for evaluating all these influences on blood concentrations and related exposure assessment. They also contribute to implementing the principles of the 3Rs in environmental risk assessment and wildlife biomonitoring. The latter because PBK models can support exposure assessment as they can provide detailed insights into the biodistribution in selected species more efficiently than conducting a large series of *in vivo* experiments. However, the applicability of PBK modelling, and thus its usefulness for risk assessment, will depend on the model complexity and quality of input parameters [45]. While it has been shown that *in vitro* models can be used to predict model parameters of absorption and metabolism, IVIVE (*in vitro* to *in vivo* exploration) always increases uncertainty in model predictions. Furthermore, high-quality *in vivo* kinetic data required for model evaluation, may not always be available, in particular in the case of agrochemicals which have typically less well-documented data than pharmaceuticals [46]. Thus, a limited number of additional *in vivo* experiments may be required for model calibration and/or evaluation.

Table 1
Physiological parameters for mouse used in the current pbk models.

Parameters	Description	imidacloprid	carbendazim	References
Vlc	Volume fraction of liver tissue	0.055		[29,48–50]
Vkc	Volume fraction of kidney tissue	0.024		
Vfc	Volume fraction of fat tissue	0.075		
Vac	Volume fraction of arterial blood	0.0185		
Vvc	Volume fraction of venous blood	0.0555		
Vrc	Volume fraction of richly perfused tissue	0.094		
Vsc	Volume fraction of slowly perfused tissue	0.678		
Pbp	Plasma-blood partitioning coefficient	0.55	0.66	Calculated from [28]
Pib	Intestine-blood partitioning coefficient	0.87	1.7577	
Plb	Liver-blood partitioning coefficient	0.87	2.3414	
Pkb	Kidney-blood partitioning coefficient	0.87	1.9029	
Pfb	Fat-blood partitioning coefficient	2.17	8.6329	
Prb	Richly perfused tissue-blood partitioning coefficient	0.87	1.7577	
Psb	Slowly perfused tissue-blood partitioning coefficient	0.48	1.7084	
QC	Cardiac output	16.5 * BW^0.74{L/h}		[29]
Qlc	Fraction of blood flow to liver	0.061		
Qkc	Fraction of blood flow to kidneys	0.091		
Qfc	Fraction of blood flow to fat	0.09		
Qsc	Fraction of blood flow to slowly perf. Tissue	0.29		
Qrc	Fraction of blood flow to rapidly perfused tissue	1-Qlc − Qkc − Qfc- Qsc		
MPPGL	Microsomal protein yield	34.5{mg/g liver}		[32–36]
S9PGL	S9 fraction protein yield	70.64 {mg/g liver}		
Ksto	Stomach emptying rate based on the average half-life of solids	0.399{/h}		
Sain	Jejunum, small intestinal surface area	3.5381{dm2}(excl. Microvilli)		
Vin	Jejunum Volume of mouse' small intestines calculated	0.00097{L}		

Once validated, also for wildlife species, PBK models could aid wildlife biomonitoring based on PBK model based reverse dosimetry of measured blood concentrations. The results of the present study reveal that this approach is feasible and at the same time illustrate aspects to be considered when designing such experiments or interpreting results. Of

Table 2
Kinetic constants for the conversion of imidacloprid and carbendazim and formation of 5-hydroxy-imidacloprid and 2-aminobenzimidazole in incubations with mouse liver microsomes, and for conversion of 5-hydroxy-imidacloprid and 2-aminobenzimidazole in incubations with mouse liver S9.

	V_{max}	Km		V_{max}	Km
imidacloprid	nmol/min/mg protein	μM	**carbendazim**	nmol/min/mg protein	μM
Microsomes depletion	3.41 ± 1.4	753 ± 422	Microsomes depletion	3.67 ± 2.1	383 ± 378
5-hydroxy-imidacloprid	nmol/min/mg protein		**2-aminobenzimidazole**	nmol/min/mg protein	
Microsomes formation	1.727 ± 1.2	2466 ± 2058	Microsomes formation	1.29 ± 0.1	33 ± 8
	nmol/min/mg S9 fraction			nmol/min/mg S9 fraction	
S9 fraction depletion	2.6 ± 0.2	85 ± 18	S9 fraction depletion	16.91 ± 2.9	369 ± 100

interest is especially that the results reveal that there will be species differences as well as differences between different model compounds that influence the accuracy of the outcomes of the blood concentration based revere dosimetry. Thus, the fold difference in the predicted steady state blood concentration and thus in the predicted external dose levels appeared to vary with i) the assumed time between dosing, which may be not well specified under wildlife conditions, ii) the catalytic efficiency for clearance of the compound of interest, and iii) the volume fraction of the liver (Vlc) of the species of interest. Low overall clearance resulting from a relatively low kcat and a relatively low Vlc will result in more stable predicted steady state levels with less fluctuations. Together this indicates that the suitability of the method for wildlife biomonitoring depends on both the species and compound of interest. The results of the present study provide some insight on what suitable values would be to allow accurate wildlife biomonitoring. It shows rats tend to be a more suitable model species than mouse because of a lower Vlc and potentially lower kcat due to lower levels of hepatic cytochromes P450, although the latter may vary with the compound of interest.

These findings underscore the necessity of considering metabolic kinetics in the early stages of method development for biomonitoring. By employing PBK-modelling, one can predict the suitability of this approach for various compounds in even more wildlife species than rats and mouse. The benchmarking against the data from rats and mouse provided in this study establishes a reference for future research and application in wildlife biomonitoring, ensuring both efficacy and reliability in environmental safety assessments. Thus, the results of this study can contribute to the development of non-invasive strategies for assessing pesticide exposure in the environment, thereby reducing the need for invasive animal testing.

CRediT authorship contribution statement

Bohan Hu: Writing – original draft, Visualization, Validation, Software, Resources, Methodology, Investigation, Formal analysis, Data curation. **Ivonne M.C.M. Rietjens:** Writing – review & editing, Supervision, Project administration, Funding acquisition, Conceptualization. **Bert Spenkelink:** Validation, Methodology, Investigation. **Nico W. van den Brink:** Writing – review & editing, Supervision, Project administration, Methodology, Funding acquisition, Formal analysis, Conceptualization.

Declaration of competing interest

The authors declare that they have no known competing financial interests or personal relationships that could have appeared to influence the work reported in this paper.

Appendix A. Supplementary data

Supplementary data to this article can be found online at https://doi.org/10.1016/j.comtox.2024.100334.

Data availability

Data will be made available on request.

References

[1] A. Sharma, V. Kumar, B. Shahzad, M. Tanveer, G.P.S. Sidhu, N. Handa, S.K. Kohli, P. Yadav, A.S. Bali, R.D. Parihar, O.I. Dar, K. Singh, S. Jasrotia, P. Bakshi, M. Ramakrishnan, S. Kumar, R. Bhardwaj, A.K. Thukral, Worldwide pesticide usage and its impacts on ecosystem. In *SN Applied Sciences* (Vol. 1, Issue 11); (2019). Springer Nature. https://doi.org/10.1007/s42452-019-1485-1.

[2] WHO - World Health Organization. (2018). Pesticide residues in Food. Retrieved April 24, 2010, at: https://www.who.int/en/news-room/fact-sheets/detail/pesticide-residues-in-food.

[3] P.C. Badgujar, S.K. Jain, A. Singh, J.S. Punia, R.P. Gupta, G.A. Chandratre, Immunotoxic effects of imidacloprid following 28 days of oral exposure in BALB/c mice, Environ. Toxicol. Pharmacol. 35 (3) (2013) 408–418, https://doi.org/10.1016/j.etap.2013.01.012.

[4] Y. Arfat, N. Mahmood, M.U. Tahir, M. Rashid, S. Anjum, F. Zhao, D.J. Li, Y.L. Sun, L. Hu, C. Zhihao, C. Yin, P. Shang, A.R. Qian, Effect of imidacloprid on hepatotoxicity and nephrotoxicity in male albino mice. Toxicology Reports, 1, (2014), 554–561. https://doi.org/10.1016/J.TOXREP.2014.08.004.

[5] S.Y. Lu, J.W. Liao, M.L. Kuo, S.C. Wang, J.S. Hwang, T.H. Ueng, Endocrine-disrupting activity in carbendazim-induced reproductive and developmental toxiclty in rats, Journal of Toxicology and Environmental Health - Part A 67 (19) (2004) 1501–1515, https://doi.org/10.1080/15287390490486833.

[6] A. Omonona, T. Jarikre, Effect of carbendazim exposure and vitamin E supplementation in African giant rats, Journal of Agriculture and Ecology Research International 4 (1) (2015) 1–9, https://doi.org/10.9734/jaeri/2015/16715.

[7] C.A. Damalas, S.D. Koutroubas, Farmers' training on pesticide use is associated with elevated safety behavior, Toxics 5 (3) (2017), https://doi.org/10.3390/toxics5030019.

[8] EC- European Commission. (2017). Guidance on monitoring and surveying of impacts of pesticide use on human health and the environment under Article 7(3) of Directive 2009/128/EC establishing a framework for Community action to achieve the sustainable use of pesticides (referred to as the Sustainable Use Directive).

[9] H. Li, M. Zhang, J. Vervoort, I.M.C.M. Rietjens, B. van Ravenzwaay, J. Louisse, Use of physiologically based kinetic modeling-facilitated reverse dosimetry of in vitro toxicity data for prediction of in vivo developmental toxicity of tebuconazole in rats, Toxicol. Lett. 266 (2017) 85–93, https://doi.org/10.1016/J.TOXLET.2016.11.017.

[10] A. Punt, M.J.W.A. Schiffelers, G. Jean Horbach, J.J.M. van de Sandt, G.M. M. Groothuis, I.M.C.M. Rietjens, B.J. Blaauboer, Evaluation of research activities and research needs to increase the impact and applicability of alternative testing strategies in risk assessment practice, Regul. Toxicol. Pharm. 61 (1) (2011) 105–114, https://doi.org/10.1016/J.YRTPH.2011.06.007.

[11] European Animal Research Association. (2017). Animal research law in the EU: Directive 201/63. Retrieved November 11, 2019, from http://eara.eu/en/animal-research/eu-animal-research-law-directive-2010-63/.

[12] E. Fabian, C. Gomes, B. Birk, T. Williford, T.R. Hernandez, C. Haase, R. Zbranek, B. van Ravenzwaay, R. Landsiedel, In vitro-to-in vivo extrapolation (IVIVE) by PBTK modeling for animal-free risk assessment approaches of potential endocrine-disrupting compounds, Arch. Toxicol. 93 (2) (2019) 401–416, https://doi.org/10.1007/s00204-018-2372-z.

[13] J. Louisse, K. Beekmann, I.M.C.M. Rietjens, Use of physiologically based kinetic modeling-based reverse dosimetry to predict in vivo toxicity from in vitro data. In *Chemical Research in Toxicology* (Vol. 30, Issue 1, pp. 114–125), (2017). American Chemical Society. https://doi.org/10.1021/acs.chemrestox.6b00302.

[14] M. Yoon, J.L. Campbell, M.E. Andersen, H.J. Clewell, Quantitative in vitro to in vivo extrapolation of cell-based toxicity assay results, Critical Reviews in Toxicology 42 (8) (2012) 633–652, https://doi.org/10.3109/10408444.2012.692115.

[15] A. Paini, J.A. Leonard, T. Kliment, Y.M. Tan, A. Worth, Investigating the state of physiologically based kinetic modelling practices and challenges associated with gaining regulatory acceptance of model applications, Regul. Toxicol. Pharm. 90 (2017) 104–115, https://doi.org/10.1016/j.yrtph.2017.08.019.

[16] H.J. Clewell, Y.M. Tan, J.L. Campbell, M.E. Andersen, Quantitative interpretation of human biomonitoring data, Toxicol. Appl. Pharmacol. 231 (1) (2008) 122–133, https://doi.org/10.1016/J.TAAP.2008.04.021.

[17] M.A. Lyons, R.S.H. Yang, A.N. Mayeno, B. Reisfeld, Computational toxicology of chloroform: reverse dosimetry using Bayesian inference, Markov chain Monte Carlo simulation, and human biomonitoring data, Environ. Health Perspect. 116 (8) (2008) 1040–1046, https://doi.org/10.1289/EHP.11079.

[18] K. Brown, M. Phillips, C. Grulke, M. Yoon, B. Young, R. McDougall, J. Leonard, J. Lu, W. Lefew, Y.M. Tan, Reconstructing exposures from biomarkers using exposure-pharmacokinetic modeling - a case study with carbaryl, Regul. Toxicol. Pharm. 73 (3) (2015) 689–698, https://doi.org/10.1016/J.YRTPH.2015.10.031.

[19] P.L. Mosquin, A.C. Licata, B. Liu, S.C.J. Sumner, M.S. Okino, Reconstructing exposures from small samples using physiologically based pharmacokinetic models and multiple biomarkers, J. Eposure Sci. Environ. Epidemiol. 19 (3) (2009) 284–297, https://doi.org/10.1038/jes.2008.17.

[20] M.L. Rigas, M.S. Okino, J.J. Quackenboss, (n.d.). Use of a Pharmacokinetic Model to Assess Chlorpyrifos Exposure and Dose in Children, Based on Urinary Biomarker Measurements. https://academic.oup.com/toxsci/article/61/2/374/1697272.

[21] Y.M. Tan, K. Liao, R. Conolly, B. Blount, A. Mason, H. Clewell, Use of a physiologically based pharmacokinetic model to identify exposures consistent with human biomonitoring data for chloroform, Journal of Toxicology and Environmental Health - Part A: Current Issues 69 (18) (2006) 1727–1756, https://doi.org/10.1080/15287390600631367.

[22] Y.M. Tan, K.H. Liao, H.J. Clewell, Reverse dosimetry: interpreting trihalomethanes biomonitoring data using physiologically based pharmacokinetic modeling, J. Eposure Sci. Environ. Epidemiol. 17 (7) (2007) 591–603, https://doi.org/10.1038/sj.jes.7500540.

[23] S. Hurst, C.M. Loi, J. Brodfuehrer, A. El-Kattan, Impact of physiological, physicochemical and biopharmaceutical factors in absorption and metabolism mechanisms on the drug oral bioavailability of rats and humans, Expert Opin. Drug Metab. Toxicol. 3 (4) (2007) 469–489, https://doi.org/10.1517/17425255.3.4.469.

[24] C.C. Travis, R.K. White, R.C. Ward, Interspecies extrapolation of pharmacokinetics, J. Theor. Biol. 142 (3) (1990) 285–304, https://doi.org/10.1016/S0022-5193(05)80554-5.

[25] E.M. Voisin, M. Ruthsatz, J.M. Collins, P.C. Hoyle, Extrapolation of animal toxicity to humans: Interspecies comparisons in drug development, Regul. Toxicol. Pharm. 12 (2) (1990) 107–116, https://doi.org/10.1016/S0273-2300(05)80052-2.

[26] J.C. Madden, G. Pawar, M.T.D. Cronin, S. Webb, Y.M. Tan, A. Paini, In silico resources to assist in the development and evaluation of physiologically-based kinetic models, Comput. Toxicol. 11 (2019) 33–49, https://doi.org/10.1016/J.COMTOX.2019.03.001.

[27] B. Hu, H.J.H.J. Van Den Berg, I.M.C.M. Rietjens, N.W. Van Den Brink, PBK models to predict internal and external dose levels following oral exposure of rats to imidacloprid and carbendazim, Comput. Toxicol. 100321 (2024), https://doi.org/10.1016/j.comtox.2024.100321.

[28] J. DeJongh, H.J.M. Verhaar, J.L.M. Hermens, A quantitative property-property relationship (QPPR) approach to estimate in vitro tissue blood partition coefficients of organic chemicals in rats and humans, Arch. Toxicol. 72 (1) (1997) 17–25, https://doi.org/10.1007/s002040050463.

[29] R.P. Brown, M.D. Delp, S.L. Lindstedt, L.R. Rhomberg, R.P. Beliles, Physiological parameter values for physiologically based pharmacokinetic models. In, Toxicol Ind Health 13 (1997) 407–484.

[30] L. Jia, H. Wong, Y. Wang, M. Garza, S.D. Weitman, Carbendazim: Disposition, cellular permeability, metabolite identification, and pharmacokinetic comparison with its nanoparticle, J. Pharm. Sci. 92 (1) (2003) 161–172, https://doi.org/10.1002/jps.10272.

[31] R.C. Kolanczyk, M.A. Tapper, B.R. Sheedy, J.A. Serrano, In vitro metabolism of imidacloprid and acetamiprid in rainbow trout and rat, Xenobiotica (2019) 1–10, https://doi.org/10.1080/00498254.2019.1694197.

[32] C. Casteleyn, A. Rekecki, A. Van Der Aa, P. Simoens, W. Van Den Broeck, Surface area assessment of the murine intestinal tract as a prerequisite for oral dose translation from mouse to man, Lab. Anim 44 (2010) 176–183, https://doi.org/10.1258/la.2009.009112.

[33] J. Lim, M.G. Miller, Role of testis exposure levels in the insensitivity of prepubertal rats to carbendazim-induced testicular toxicity, Fundam. Appl. Toxicol. 37 (2) (1997) 158–167, https://doi.org/10.1006/FAAT.1997.2315.

[34] R.J. Qasem, J.K. Fallon, M. Nautiyal, M. Mosedale, P.C. Smith, Differential detergent fractionation of membrane protein from small samples of hepatocytes and liver tissue fcor quantitative proteomic analysis of drug metabolizing enzymes and transporters, J. Pharm. Sci. 110 (1) (2021) 87–96, https://doi.org/10.1016/j.xphs.2020.10.037.

[35] R. Schwarz, A. Kaspar, J. Seelig, B. Kü, Gastrointestinal Transit Times in Mice and Humans Measured With 27 Al and 19 F Nuclear Magnetic Resonance, (2002). https://doi.org/10.1002/mrm.10207.

[36] K. Słoczyńska, A. Gunia-Krzzyzak, P. Koczurkiewicz, K. Wojcik-Pszczola, D. Zelaszczyk, J. Popiol, Metabolic stability and its role in the discovery of new chemical entities, Acta Pharm 69 (2019) 345–361, https://doi.org/10.2478/acph-2019-0024.

[37] R. Abdullah, W. Alhusainy, J. Woutersen, I.M.C.M. Rietjens, A. Punt, Predicting points of departure for risk assessment based on in vitro cytotoxicity data and physiologically based kinetic (PBK) modeling: The case of kidney toxicity induced by aristolochic acid I. *Food and Chemical Toxicology*, *92,* (2016), 104–116. .

[38] Q. Wang, B. Spenkelink, R. Boonpawa, I.M.C.M. Rietjens, K. Beekmann, Use of physiologically based kinetic modeling to predict rat gut microbial metabolism of the isoflavone daidzein to S-equol and its consequences for ERα activation, Mol. Nutr. Food Res. 64 (6) (2020), https://doi.org/10.1002/MNFR.201900912.

[39] X. Cheng, K.X. Chen, N.D. Jiang, L. Wang, H.Y. Jiang, Y.X. Zhao, Z.L. Dai, Y.J. Dai, Nitroreduction of imidacloprid by the actinomycete Gordonia alkanivorans and the

stability and acute toxicity of the nitroso metabolite, Chemosphere 291 (P2) (2022) 132885, https://doi.org/10.1016/j.chemosphere.2021.132885.
[40] U. Kapoor, M.K. Srivastava, P. Trivedi, V. Garg, L.P. Srivastava, Disposition and acute toxicity of imidacloprid in female rats after single exposure, Food Chem. Toxicol. 68 (2014) 190–195, https://doi.org/10.1016/j.fct.2014.03.019.
[41] N. Mencke, P. Jeschke, Therapy and prevention of parasitic insects in veterinary medicine using imidacloprid, Curr. Top. Med. Chem. 2 (7) (2005) 701–715, https://doi.org/10.2174/1568026023393598.
[42] Y. Sun, C. Huang, Y. Jiang, Y. Wan, Urinary concentrations of fungicide carbendazim's metabolite and associations with oxidative stress biomarkers in young children, Environ. Sci. Pollut. Res. (2022), https://doi.org/10.1007/s11356-022-23311-2.
[43] J.J.P. Bogaards, M. Bertrand, P. Jackson, M.J. Oudshoorn, R.J. Weaver, P.J. Van Bladeren, B. Walther, Determining the best animal model for human cytochrome P450 activities: a comparison of mouse, rat, rabbit, dog, micropig, monkey and man, Xenobiotica 30 (12) (2000) 1131–1152, https://doi.org/10.1080/00498250010021684.
[44] M.L. Chen, L. Lesko, R.L. Williams, Measures of exposure versus measures of rate and extent of absorption, Clin. Pharmacokinet. 40 (8) (2001) 565–572, https://doi.org/10.2165/00003088-200140080-00001.
[45] A. Paini, J.V. Sala Benito, J. Bessems, A.P. Worth, From in vitro to in vivo: Integration of the virtual cell based assay with physiologically based kinetic modelling, Toxicol. In Vitro 45 (2017) 241–248, https://doi.org/10.1016/J.TIV.2017.06.015.
[46] R. Jiang, J. Shen, X. Li, R. Gao, Q. Zhao, Z. Su, Detection and recognition of veterinary drug residues in beef using hyperspectral discrete wavelet transform and deep learning, Int. J. Agric. Biol. Eng. 15 (1) (2022) 224–232, https://doi.org/10.25165/j.ijabe.20221501.6459.
[47] J. Krechniak, B. Kłosowska, The fate of 14c-carbendazim in rat, Xenobiotica 16 (9) (1986) 809–815, https://doi.org/10.3109/00498258609038962.
[48] E.L. Bradshaw-Pierce, S.G. Eckhardt, D.L. Gustafson, A physiologically based pharmacokinetic model of docetaxel disposition: from mouse to man, Clin. Cancer Res. 13 (9) (2007) 2768–2776, https://doi.org/10.1158/1078-0432.CCR-06-2362.
[49] D.J. Marino, H.J. Clewell, P.R. Gentry, T.R. Covington, C.E. Hack, R.M. David, D. A. Morgott, Revised assessment of cancer risk to dichloromethane: Part I Bayesian PBPK and dose-response modeling in mice, Regul. Toxicol. Pharm. 45 (1) (2006) 44–54, https://doi.org/10.1016/J.YRTPH.2005.12.007.
[50] J. Ning, L. Chen, M. Strikwold, J. Louisse, S. Wesseling, I.M.C.M. Rietjens, Use of an in vitro–in silico testing strategy to predict inter-species and inter-ethnic human differences in liver toxicity of the pyrrolizidine alkaloids lasiocarpine and riddelliine, Arch. Toxicol. 93 (3) (2019) 801–818, https://doi.org/10.1007/s00204-019-02397-7.